MULTI-DISCIPLINARY SYSTEM DESIGN OPTIMIZATION OF THE F-350 REAR SUSPENSION*†

Jacob Wronski
Master of Science Candidate
Department of Mechanical Engineering
MIT CADlab

J. Michael Gray
Master of Science Candidate
Department of Mechanical Engineering
MIT CIPD

ABSTRACT

This paper presents how a Multi-Disciplinary System Design Optimization (MSDO) approach can be implemented to optimize the performance of the F-350 Ford truck rear suspension subsystem. The MSDO approach encompasses five phases: a problem and system definition phase, a numerical simulation phase, a design space exploration phase, a single objective optimization phase, and a multi-objective optimization phase. Each of these phases is presented within the specific context of the design and performance of the F-350 Ford truck rear suspension. The suspension system was defined using seven design variables, twelve fixed parameters, six constraints and two objectives. The overall objective, to maximize suspension performance, was measured in terms of "passenger comfort" which was in turn based primarily on the maximum acceleration experienced by the passenger cabin. For multi-objective optimization, the settling time of the passenger cabin was added as a second measure of passenger comfort. Using this system definition, a numerical simulation of the suspension was created in Matlab®. An orthogonal array was used to determine an initial starting point for full optimization. Both gradient-based and heuristic-based optimization techniques are employed as well as a weighted multi-objective technique. The results of these efforts are presented and some conclusions are drawn.

INTRODUCTION

Motivation

When a customer buys a vehicle, there are many factors he/she considers. Among these are cost, gas mileage, safety, and the "smoothness" of the ride. It is well known that the design of the suspension affects all of these factors. To illustrate, a poorly designed suspension may result in any of the following situations that directly relate to the factors above: a rough ride over certain road conditions, catastrophic failure of the axle under certain loading conditions, fuel inefficiency due to excess weight, and increased sticker price due to the use of unnecessarily expensive components. A good design theoretically would avoid all these situations. However, this can be difficult to achieve in practice.

Approach

In an effort to reduce the difficulty associated with suspension design, a Multidisciplinary Design Optimization (MSDO) approach was used. Specifically, it was applied to the design of the rear suspension of the F-350 Ford truck. Figure 1 shows the architecture of this suspension.

---

*In Collaboration with Ford Motor Company.

Figure 1. CAD Model of the F-350 Rear Suspension.

Paper Outline

The remainder of this paper proceeds as follows. First, a formal definition both the system and the problem are presented. Second, the numerical simulation of the physical system is discussed. Next follows a discussion of the initial design space exploration process. Fourth, the setup and results of single objective optimization are presented for both gradient-based and heuristic-based search methods. Next, the results from a multi-objective optimization technique are explored. Finally, conclusions drawn from the results are mentioned with a brief discussion of future work.

PROBLEM AND SYSTEM DEFINITION

The design problem being addressed is related to the optimization of the performance of the F-350 Ford truck rear suspension. This suspension system was defined in four ways. First, it was defined by several design variables. These are design characteristics that can be changed by the designer within certain bounds. Second, it was defined by a set of fixed parameters. These are those design characteristics that cannot be changed by the designer. Third, constraints were used to define the system. These are limitations that the suspension design is subject to or minimum performance criteria that the design must meet. Finally, system objectives were defined. These are characteristics by which the performance of the suspension was measured. Each of these four areas of system definition is now addressed.

Design Variables

The chosen design variables are all real, continuous, bounded numbers and are shown in Table 1. Also, only the damping coefficient of the shock absorber, C_s, is not a geometric characteristic. These characteristics were chosen as design variables because it was felt that a suspension designer would have liberty to change them within certain bounds. The decision was also motivated by the fact that the design variables mostly represent the geometry of the suspension design, and changes in this geometry are an easy thing to visualize and understand.

Fixed Parameters

The fixed parameters for the suspension are shown in Table 2. These include material properties, overall vehicle and tire dimensions, road surface parameters and physical constants. These were characteristics of the system that were assumed to be out of control of the designer.

Table 1. Design Variables.

Symbol	Description	Units	Nominal Value	Lower/Upper Bounds
L_s	length of leaf spring	m	1	$1 <= L_s <= 1.5$
h_s	thickness of leaf spring	m	0.005	$.005 <= h_s <= .025$
b_s	width of leaf spring	m	0.1	$.05 <= b_s <= .125$
t_a	thickness of axle tube	m	0.1	$.05 <= t_a <= .015$
d_a	outer diameter of axle tube	m	0.125	$.075 <= d_a <= .150$
L_a	bending length of axle	m	0.6	$0.5 <= L_a <= 0.7$
C_s	damping coefficient of shock absorber	Ns/m	1500	$500 <= C_s <= 5000$

Table 2. Fixed Parameters.

Symbol	Description	Units	Value
E	Modulus of Elasticity, steel	Pa	$206x10^9$
ω_i	Road bump frequency	rad/s	12.57
m_c	Mass of passenger cabin	kg	1800
g	gravity constant	m/s^2	9.81
d_w	diameter of the wheel	meters	0.5
u	tire on cement sliding friction coeffient	Unitless	0.6
F_t	Road bump height	meters	0.1
K_t	Stiffness of Tire	N/m	160000
ρ	density of steel	kg/m^3	7850
S_f	Stress safety factor	Unitless	2
L	half length of axle	meters	0.92
m_t	Mass of the tire	kg	18

Constraints

Table 3 lists the intermediate variables of the suspension design that were either subject to constraints or were needed for the calculation of the objectives. Note that while the settling time, S_t, is listed here as being subject to a constraint, it is later treated as a second objective in the multi-objective optimization phase of MSDO. There are also a constraint on cost, gas mileage, internal axle stress, and the natural frequency ratio of the mass of the suspension and the mass of the passenger cabin.

Table 3. Intermediate or Constrained Variables.

Symbol	Description	Units	Constraint
m_s	Mass of Suspension Parts	kg	None
K_s	Spring Stiffness	N/m	None

Objectives

Table 4 shows the objective for single objective optimization. The overall objective of this optimization design is to maximize the passenger comfort inside the automobile cabin. After careful consideration it was decided that passenger comfort would be defined in numerical terms as the vertical acceleration of the passenger cabin caused by the vehicle driving over a road bump. The single objective optimization problem was to minimize this acceleration.

Table 4. Single Optimization Objective.

Symbol	Description	Units
Min [a_{max}]	Minimize maximum acceleration experienced by passenger cabin	m/s^2

In the last phase of MSDO a second objective was introduced, namely the settling time, $\boldsymbol{S_t}$. Settling time is also an important measure of overall comfort in the passenger cabin as it represents how long the cabin oscillates after a road disturbance has been cleared. A long oscillation period may be very uncomfortable to the passengers inside just as high accelerations are. For this reason it was chosen as the second objective.

NUMERICAL SIMULATION

In order to use the MSDO methodology, a numerical simulation of the behavior of the physical system must be created. This was done using the system definition described above to create a set of linked multidisciplinary modules that simulate the behavior of the system. In this case, there were six modules, one for each of the following aspects of the design: the dynamics, the stiffness of the leaf spring, the axle internal stresses, the suspension mass, the cost, and the gas mileage. Each of these modules will now be discussed.

The Dynamic Module

The dynamic behavior of the F-350 rear suspension was modeled using a 4th order quarter-car suspension model consisting of springs, masses, and dampers (see Figure 2) [1]. To simulate the road disturbance, a step input function, $\boldsymbol{F_t}$, of 0.1 meters was used to simulate a large "bump" [2]. Critical model inputs are: (i) the passenger cabin and suspension mass, $\boldsymbol{m_c}$ and $\boldsymbol{m_s}$, (ii) the leaf spring and tire stiffness, $\boldsymbol{K_s}$ and $\boldsymbol{K_t}$, and (iii) the damping coefficient of the suspension damper, $\boldsymbol{C_s}$. Since the damping coefficient of the tire, $\boldsymbol{C_t}$, was negligible in relation to the rest of the system it was not included in this analysis. The outputs of this model are the settling time, $\boldsymbol{S_t}$, the maximum cabin acceleration $\boldsymbol{a_{max}}$, and the natural frequency ratio, $\boldsymbol{\omega_{ratio}}$ between the two masses.

To validate the dynamics module, the vertical displacement response of $\boldsymbol{m_s}$ when subject to a 0.1 meter step road disturbance, $\boldsymbol{F_t}$, was compared to the results found in [1] for an identical situation. The two responses matched to within about 5%.

The Leaf Spring Stiffness Module

The leaf spring was modeled as a steel prismatic bar obeying Hooke's law [3]. The boundary conditions were a simple support on each end with a single centered point load $\boldsymbol{F_s}$ (see Figure 3). Inputs for this module are the dimensions of the leaf spring, $\boldsymbol{L_s}$, $\boldsymbol{h_s}$, and $\boldsymbol{b_s}$, and $\boldsymbol{E}$, the modulus of elasticity of steel. The output of this module is the leaf spring stiffness, $\boldsymbol{K_s}$, which is found from the following equation:

$$K_s = \frac{F_s}{\delta_s} = \frac{48EI_s}{L_s^3} = \frac{4Eb_sh_s^3}{L_s^3} \tag{1}$$

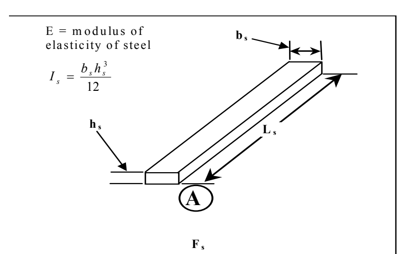

The Axle Internal Stress Module

The axle was modeled as tubular beam with simple supports at each end [3]. The passenger compartment resting on the axle was modeled as two equal and symmetrically located point loads $\boldsymbol{F_a}$ (see Figure 4). The inputs for this module are the location of the loads from the ends of the beam, $\boldsymbol{F_a}$, and the dimension of the axle, $\boldsymbol{t_a}$ and $\boldsymbol{d_a}$. The output of this module is the maximum internal stress, $\boldsymbol{\Omega_{max}}$. To find $\boldsymbol{\Omega_{max}}$, the bending, shear, and torsion stresses due to the combination of the weight of the passenger cabin and the dynamic loading were calculated from the following equations respectively:

$$\sigma_{\max} = \frac{M_{\max} d_a}{2I_a} = \frac{8m_c(g + a_{\max})d_a}{\pi\left(d_a^4 - (d_a - 2T_a)^4\right)} \quad (2a)$$

$$\nu_{\max} = \frac{4V}{A_c} = \frac{2m_c(g + a_{\max})}{\pi d_a^2} \quad (2b)$$

$$\tau_{\max} = \frac{Td_a}{2J_a} = \frac{4m_c(g + a_{\max})d_w \mu}{\pi\left(d_a^4 - (d_a - 2T_a)^4\right)} \quad (2c)$$

Then, using Mohr's circle [3] and the stresses above, maximum internal stress of the axle, $\boldsymbol{\Omega_{max}}$, can be found from the following equation:

$$\Omega_{\max} = \max[Z_1, Z_2] \quad (3a)$$

$$where\ Z_1 = \frac{\sigma_{\max}}{2} + \left(\frac{\sigma_{\max}^2}{4} + \tau_{\max}^2\right)^2 \quad (3b)$$

$$and\ \ Z_2 = \tau_{\max} + \nu_{\max} \quad (3c)$$

The Suspension Mass Module

This simple but important module is used to calculate the mass of the suspension, $\boldsymbol{m_s}$, based on the part dimensions and material densities obtained directly from the CAD geometry of the suspension. The CAD model representation of the F-350 suspension system is native to I-DEAS Version 8 and is shown in Figure 5. This output is used in several other modules.

The physical suspension is composed of a three-piece leaf spring and a damper attached to a hollow axle. To obtain the suspension mass, the I-DEAS model was parametrically driven using five design variables and one fixed parameter: (i) the leaf spring length, $\boldsymbol{L_s}$, (ii) the leaf spring width, $\boldsymbol{b_s}$, (iii) the leaf spring thickness, $\boldsymbol{h_s}$, (iv) the shaft diameter, $\boldsymbol{d_a}$, (v) the shaft wall thickness, $\boldsymbol{t_a}$, and (vi) the density of steel, $\boldsymbol{\rho}$. DOME™, a program that links CAD models to other simulation codes such as Matlab® and was developed at the MIT CADlab, was used to link this module to the other modules.

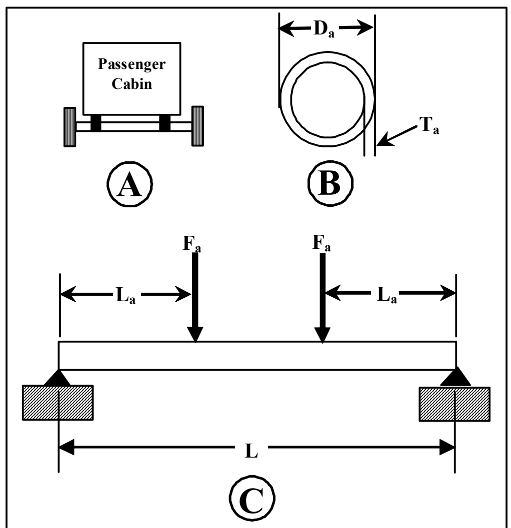

Figure 4. A) Rear view of truck, B) axle cross section, and C) front view of axle.

Figure 5. CAD model of F-350 rear suspension.

Gas Mileage Module

The gas mileage module is a placeholder module based on data of other vehicles in the same class. Gas mileage, ***GM***, is given by the following equation using the mass of the suspension, $\boldsymbol{m_s}$, as input:

$$GM = 25 - 0.075 \times (4 \times m_s) \tag{4}$$

This model calculates the energy consumption of the proposed suspension design and as such introduces environmental liability in this multi-disciplinary optimization problem.

Cost Module

Since the actual cost of the F-350 rear suspension system was not known, a simple polynomial expression was used to estimate a reasonable cost in this study. Inputs are the masses of the car and suspension, $\boldsymbol{m_c}$ and $\boldsymbol{m_s}$, the bending lengths of the axle and leaf springs, $\boldsymbol{m_c}$ and $\boldsymbol{m_s}$, and the damping coefficient of the shock absorber. The cost, ***C***, of the suspension is given by:

$$C = y_1(m_c + 4 \times m_s) + y_2\left(\frac{1}{C_s}\right)^2 + y_3 L_a^{\,2} + y_4 L_s^{\,3} \tag{5}$$

$$where\ \ y_1 = y_2 = y_3 = y_4 = 1$$

The complete numerical simulation of the suspension was created by the inputs and outputs of all six modules as shown in Figure 6. It is interesting to note that there are no feedback loops in the simulation.

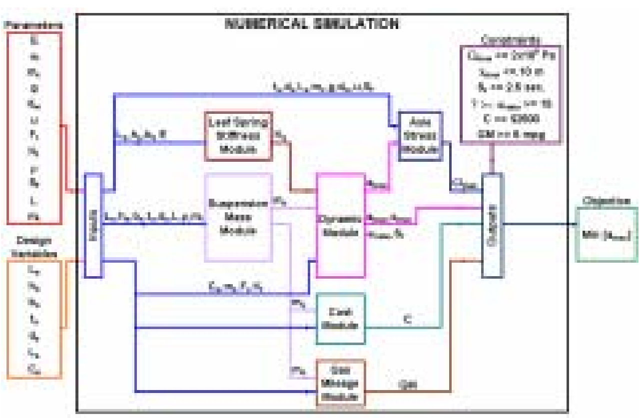

Figure 6. The Completed Simulation with Six Linked Modules.

DESIGN SPACE EXPLORATION

Before beginning any rigorous optimization, an L_{18} orthogonal array of seven design variables with three levels was used to explore the design space. From this array of experiments, an initial design vector $\boldsymbol{X_o}$, was chosen that had the lowest objective value, $\boldsymbol{a_{max}}$, without violating any of the constraints. This initial design vector appears in the left side of Figure 7. Then, by calculating the diagonal entries of the Hessian, $\boldsymbol{X_o}$ was scaled so that all the design variables were roughly on the same order of magnitude. This scaled design vector is shown in Figure 7 on the right as $\boldsymbol{X_{os}}$.

$$X_o = \begin{bmatrix} L_s \\ h_s \\ b_s \\ t_a \\ d_a \\ L_a \\ C_s \end{bmatrix} = \begin{bmatrix} 1.00 \\ .005 \\ .100 \\ .010 \\ .125 \\ .5 \\ 1500 \end{bmatrix} \qquad X_{os} = \begin{bmatrix} L_s \\ h_s \\ b_s \\ t_a \\ d_a \\ L_a \\ C_s \end{bmatrix} = \begin{bmatrix} 1.25 \\ 0.5 \\ 1.0 \\ 1.0 \\ 1.25 \\ .6 \\ 1.5 \end{bmatrix}$$

Before **After**

Figure 7. The Design Vector Before and After Ccaling.

SINGLE OBJECTIVE OPTIMIZATION

Gradient-Based Search

With the MSDO framework established and an initial design vector chosen, formal optimization can now be executed. Initially, the Quasi-Newton, SQP gradient search embodied in the "fmincon" function in Matlab® was used to optimize the design. The search was executed by starting with both the scaled and unscaled initial design vectors and the results are shown in Table 5. Matlab® reported that both runs converged successfully. This means that the Karush-Kuhn-Tucker (KKT) conditions are satisfied within the default tolerance of 0.001 at the optimum solution. It is clear from Table 5 that although both runs converged to the same objective value of $\boldsymbol{a_{max}}$, J($\boldsymbol{X^*}$), the search converged much quicker (more than 2.5 times) when starting with the scaled initial design vector.

Table 5. Effects of Scaling on J(X^*) and Elapsed Time.

Run Description	J(X^*) (m/s^2)	Elapsed Time (s)
Unscaled, (X_o)	10.954	16.174
Scaled, (X_{os})	10.954	6.079

Comparing the design vector before and after optimization (using the scaled initial design vector), several things can be noted (see Table 6). First, $\boldsymbol{L_a}$, remains unchanged. This is because $\boldsymbol{L_a}$ only affects the internal stress in the axle and while it is not apparent now, we will see later that the constraint on the internal stress is not active at the optimal solution. Second, at the optimal solution, $\boldsymbol{t_a}$ and $\boldsymbol{d_a}$ are near their upper bounds thus resulting in a bigger axle and heavier suspension. This is most likely due to the fact that heavier suspensions result in lower cabin accelerations and lower internal stresses, both desirable effects in this case. Of course, a heavier suspension also means a lower gas mileage rating. We will see later that the gas mileage constraint is active at the optimum. Third, $\boldsymbol{h_s}$ is near its lower bound. This probably due to the fact that a thinner leaf spring will have a smaller lower stiffness thereby reducing passenger cabin accelerations. Finally, $\boldsymbol{a_{max}}$, was reduced by 23%, a significant improvement. Of course, there is no guarantee that this search found the globally optimal solution, but it has clearly found a local optimum (since the KKT conditions are met) and it represents a modest improvement over the best solution found with the orthogonal array. For a visual representation of this improvement, Figure 8 shows the vertical acceleration of the passenger cabin, $\boldsymbol{a}$, as a function of time, both before and after optimization. $\boldsymbol{a_{max}}$ occurs after about .025 seconds at the peak of the first oscillation.

Table 6. Optimization Results: Design Variables & Objective

Design (scaled)	L_s	h_s	b_s	t_a	d_a	L_a	Cs	$J(x)=a_{max}$
Before Optimization	1.00	0.500	1.00	1.0	1.25	0.600	1.5	**14.290**
After Optimization	1.380	0.511	1.216	1.500	1.5	0.600	1.317	**10.954**

Table 6. The Initial and Optimum Design Vectors.

Design	L_s	h_s	b_s	t_a	d_a	L_a	Cs	J(X), a_{max}
Initial, (X_{os})	1.00	0.50	1.00	1.0	1.25	0.60	1.50	**14.290**
Optimum, (X*)	1.38	0.51	1.22	1.50	1.50	0.60	1.32	**10.954**

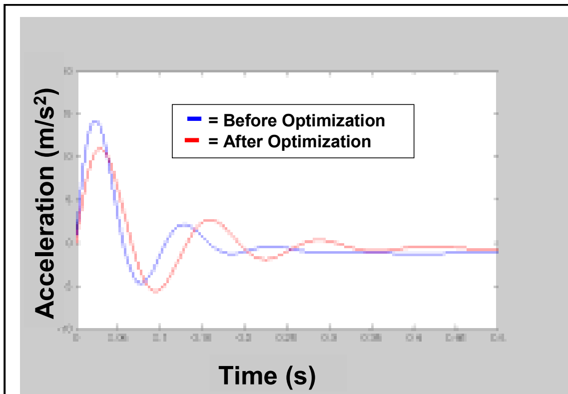

Figure 8. The Vertical Acceleration of the Passenger Cabin Before and After Optimization.

Heuristic-Based Search

In addition to using a Quasi-Newton gradient search, two heuristic techniques were executed for comparison: a Simulated Annealing algorithm (SA), and a Genetic Algorithm (GA). Both of these heuristic methods were executed in iSight® using the same initial scaled design vector, $\boldsymbol{X_{os}}$, shown in Figure 7. The results of these optimization runs are shown in Tables 7 and 8. The results from the gradient search are also shown in these tables for comparison. The SA was set to converge when the search resulted in five consecutive identical designs. Convergence for the GA was based on the number of generations, which was set to 50 in this case.

Table 7. The Optimum Design Vectors Obtained by All Three Search Methods.

Run Type	L_s	h_s	b_s	t_a	d_a	L_a	Cs	J(X*), a_{max}
SA, (X*)	1.49	0.62	0.90	1.50	1.48	0.50	1.32	**11.040**
GA, (X*)	1.47	0.61	0.93	1.50	1.50	0.57	1.32	**11.038**
SQP, (X*)	1.38	0.51	1.22	1.50	1.5	0.60	1.32	**10.954**

Table 8. The Constrained Module Outputs and Elapsed Times for the Three Search Methods.

Run Type	Ω_{max} (MPa)	GM (mpg)	S_t (s)	ω_{ratio}	C ($)	xc_{max} (m)	Elapsed Time (s)
SA	50.21	5.23	2.49	14.80	2067.16	0.086	**420**
GA	56.12	5.08	2.49	14.55	2069.19	0.083	**840**
SQP	58.10	5.00	2.50	15.00	2070.00	0.092	**6**

Looking at Table 7, it can be seen that the gradient search found a better solution than either of the two heuristic techniques although all three found designs with similar performance. The most striking difference between the three search methods is in the elapsed time. The SA took 70 times as long and the GA took 140 times as long as the SQP method. It is clear that for at least this design problem, the gradient technique was both faster and more successful.

Objective Sensitivity Analysis

Once the optimal design vector, $\boldsymbol{X^*}$, was calculated, the sensitivity of the objective function with respect to the design variables around the optimal point was investigated.

Normalized sensitivities of the objective function with respect to each design variable were obtained using the finite difference approach. The calculated sensitivities are shown in Figure 9.

It is clear from Figure 9 that the objective function was most sensitive to the damping coefficient of the shock absorber, C_s. Since the objective was to **minimize** the maximum vertical acceleration of the passenger cabin, a_{max}, any increase in the damping coefficient would have resulted in a worse design. Those with knowledge of suspension design may have been able to anticipate this result.

It can also be seen from Figure 9 that any increase in the outer diameter of the axle, d_a, the thickness of the axle tube, t_a, and the length of the leaf spring, L_s, would improve the objective. This is to be expected since they all increase the weight of the suspension and heavier suspensions are not as sensitive to road conditions. However, these changes come with a price. Increasing the weight of the suspension also has some undesirable side effects. More on this trade off between performance and weight will be highlighted later.

From Figure 9, it can also be seen that objective function is insensitive to the location of the attach point of the passenger cabin to the axle, L_a, This is due to the fact that L_a, only affects the internal stresses of the axle and not the weight or dynamic properties of the suspension.

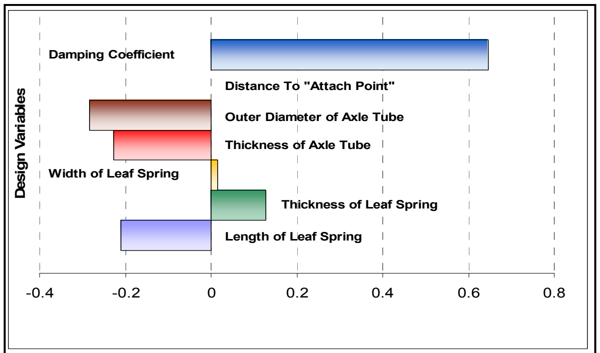

Figure 9. Sensitivity of J(X*) With Respect to the Design Variables.

Parameter Sensitivity Analysis

The sensitivity of the optimum design vector X^* was investigated with respect to the following fixed parameters: the material density, ρ, the mass of the car, m_c, and the car tire stiffness, K_t. A forward difference approximation was used to calculate $\delta p/\delta X$ for each of the seven design variables. This was accomplished by calculating $\Delta p/\Delta X$ for 14 different perturbation step sizes, Δp, ranging from 0.1%-10% of the nominal value of each fixed parameter. This data was used to determine the perturbation range over which the linear approximation made when using a finite differencing method is valid. The best step size was chosen for each case and the results are summarized in Table 9.

Table 9. Sensitivity of X* With Respect to Three of the Fixed Parameters.

	Design Variables						
Parameter	$\Delta L_s/\Delta p$	$\Delta b_s/\Delta p$	$\Delta h_s/\Delta p$	$\Delta t_a/\Delta p$	$\Delta d_a/\Delta p$	$\Delta L_a/\Delta p$	$\Delta C_s/\Delta p$
ρ (Material Density)	-6.20E-04	-2.40E-06	-1.00E-06	-2.00E-07	-1.00E-05	0.0	0.0
m_c (Mass of Car)	2.00E-04	6.00E-07	0.0	0.0	0.0	0.0	7.80E-04
K_t (Tire Stiffness)	1.50E-06	6.00E-09	0.0	0.0	0.0	0.0	0.0

It can be seen from Table 9 that an increase in the material density will result in a decrease in all but 2 of the design variables. This is because these two design variables, L_a and C_s, are not related to the material density in any of the modules in the simulation and therefore their sensitivities with respect to the material densities are both zero. From Figure 9 it is also evident that L_s, h_s, and C_s are sensitive to changes in the mass of the car (passenger cabin). This is because changes in the mass of the car affect the dynamic properties of the system and the spring dimensions and shock absorber damping properties must compensate. Similarly, when K_t is changed, the spring dimensions must change to accommodate.

Constraint Sensitivity Analysis

Calculations revealed that three of the 6 constraints are active at X^*. They are the lower limit on GM (gas mileage), and the upper limits on ω_{ratio} (natural frequency ratio) and S_t (settling time). Notice that the maximum internal stress, Ω_{max}, is not active at the optimum. The Lagrange multipliers, λ, for the active constraints represent the sensitivity of $J(X^*)$ to these constraints. Table 10 shows the Lagrange multipliers for the three active constraints. It can bee seen that Settling time is the most important active constraint.

Table 10. Lagrange multipliers of the Three Active Constraints at X^*.

Active Constraint	λ
GM (gas mileage)	1.223
S_t (settling time)	7.069
ω_{ratio} (natural frequency ratio)	1.551

In fact, moving the minimum settling time constraint from a value of 2.5 to 5.0 seconds allows the objective function to change from 10.95 m/s^2 to 6.87 m/s^2. This significant improvement confirms the importance of this constraint to the minimization of the maximum vertical acceleration of the passenger cabin. For the last phase of MSDO, this constraint was lifted and settling time was treated as a second objective.

MULTI-OBJECTIVE OPTIMIZATION

In the previous phases, the focus was on design optimization relative to a single objective. Since maximizing passenger comfort when traveling over rough terrain was the overall goal, minimizing a_{max} was a suitable objective. However, another factor that is important to passenger comfort relating to the suspension is the amount of time that the passenger cabin continues to oscillate after the rough terrain has been passed. This is often called settling time. A suspension that optimizes overall passenger comfort would really take this into account in addition the vertical acceleration. Thus settling time, S_t, was chosen as a second objective.

Pareto Front Creation

To create a Pareto front for the multi-objective problem described above, a weighted sum approach was used. The new objective has the following form:

$$\begin{aligned} &\min[J_i(X)] \\ &where\ J_i(X) = (1-w_i)\times(a_{\max}) + w_i \times (S_t) \\ &0 < w_i < 1 \\ &w_{i+1} - w_i = 0.1 \end{aligned} \tag{6}$$

Since a_{max} and S_t are positive quantities, there is no danger of the two canceling each other out in the composite objective. In addition to the nine weighting factors listed in the formulation above (0.1, 0.2, …, 0.9) , .01, .99, and .85 were also included to make the Pareto front more complete. The Pareto front is shown in Figure 10 below. The data is shown in Table 11 (all values are scaled).

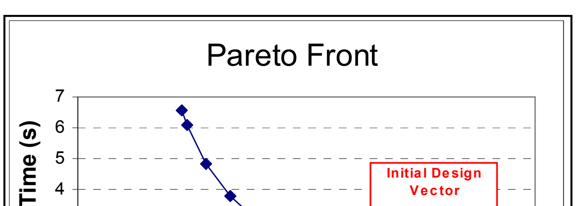

Table 11. The Pareto Front Data.

w_i	a_{max}	S_t	L_s	h_s	b_s	t_a	d_a	L_a	C_s
0.01	5.70	6.58	1.50	0.55	1.23	1.50	1.46	0.50	**0.50**
0.10	5.70	6.58	1.50	0.55	1.24	1.50	1.46	0.50	**0.50**
0.20	5.70	6.58	1.49	0.55	1.24	1.49	1.47	0.50	**0.50**
0.30	5.70	6.58	1.50	0.55	1.24	1.49	1.48	0.50	**0.50**
0.40	6.01	6.09	1.49	0.55	1.20	1.49	1.48	0.50	**0.54**
0.50	7.03	4.83	1.46	0.55	1.17	1.49	1.49	0.50	**0.68**
0.60	8.34	3.77	1.41	0.53	1.15	1.50	1.50	0.50	**0.87**
0.70	10.09	2.84	1.41	0.53	1.15	1.50	1.50	0.50	**1.16**
0.80	12.87	1.93	1.43	0.55	1.13	1.50	1.50	0.50	**1.71**
0.85	15.65	1.45	1.50	0.57	1.15	1.49	1.48	0.50	**2.27**
0.90	18.96	0.92	1.50	0.56	1.16	1.46	1.50	0.50	**3.56**
0.99	21.68	0.66	1.45	0.57	1.05	1.50	1.50	0.50	**5.00**

By looking at the Pareto front, several things can be noted. First, the only design variable that undergoes a significant change as one moves up and down the Pareto front is, C_s, the damping coefficient of the shock absorber. This means that this design variable is the one that should be adjusted to convert a suspension with high accelerations but short settling times to one with low accelerations but high settling times. Second, for weighting factors between .01 and .3, there was no change in the values of the individual objective functions. This is because the damping coefficient, C_s, reached its lower bound of .5 (or 500 N/m when not scaled

From the Pareto front we can also see that initial design vector found by using the orthogonal array was close to Pareto-optimal. Also, the design found using single objective optimization is also on the Pareto front and is close to the initial design vector. This may be a reason that the SQP method was so effective and the runtime was short.

Figures 11 and 12 show the vertical acceleration and displacement of the passenger cabin for two designs: one generated by minimizing the settling time, S_t (shown in red), and one created by minimizing the vertical acceleration, a_{max} (shown in blue). It is clear that the two designs have very different behavior. When minimizing the settling time is the dominant objective, the result is a design that stops oscillating in less than one second after climbing the 0.1 meter road disturbance, but also experiences an acceleration of over 20 m/s^2 (see Figure 11). When minimizing the acceleration is the dominant objective, the result is a design that oscillates for more than six seconds but only experiences an acceleration of 5.7 m/s^2 (see Figure 12).

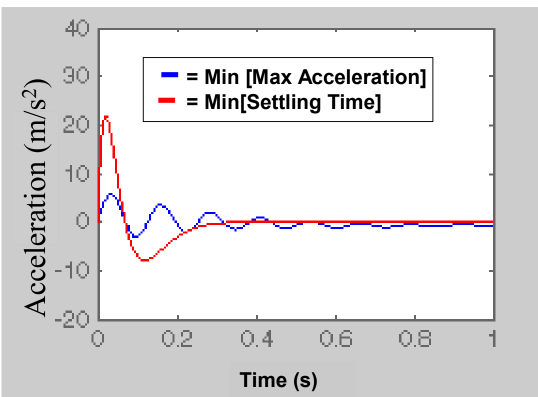

Figure 11. The Passenger Cabin Acceleration as a Function of Time.

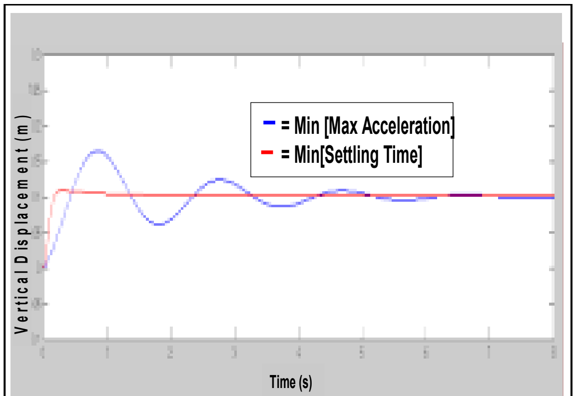

Figure 12. The Passenger Cabin Displacement as a Function of Time.

CONCLUSIONS AND FUTURE WORK

In this paper, an MSDO approach has been used to optimize the performance of the F-350 rear truck suspension. Single- and multi-objective optimization methods were used in conjunction with a numerical simulation to find the design with the optimal performance. It was found that heavier suspensions with low stiffness resulted in lower vertical cabin accelerations. Settling time can also be reduced by increasing the damping coefficient of the shock absorber (i.e. using a more viscous oil). However, this reduction comes at the expense of increased vertical accelerations of the passenger cabin.

In the future, the authors hope to look closer at the tradeoffs between the maximum acceleration and other potential objectives such as cost or gas mileage. It is anticipated that more of the design variables will change significantly when making trading-offs between these dissimilar objectives.

We also hope to continue to improve the fidelity of the numerical simulation so that it captures more of the behavior of the actual F-350 truck rear suspension. As part of this, we hope to include more road conditions in addition to the 0.1 meter step input.

Another area of future work involves the simulation linking software DOME™. The authors foresee that with DOME, each module of the simulation could be characterized in a different software package that is most suitable for the particular discipline. For example, an FEA software package could be used in to measure the stiffness of the leaf spring and the internal stresses in the axle more accurately than the simple Matlab® code used for the simulations in this paper. Cost and gas mileage modules could be put into Excel. Then, DOME™ could be used to seamlessly link all these modules together. DOME™ also would make it easy for more modules to be added later, such as modules for noise, handling, and alignment.

REFERENCES

[1] Wong, Jo Yung, *Theory of Ground Vehicles,* New York, John Wiley, 2001.

[2] Hyniova, Katerina, A. Stribrsky, and J. Honcu, "Fuzzy Control of Mechanical Vibrating Systems", *Proceedings of International Carpathian Control Conference*, 1993.

[3] Norton, Robert L., *Machine Design: An Integrated Approach*, New Jersey, Prentice-Hall, 2000.